Inorganic Chemistry

Article

pubs.acs.org/IC

Gas Sorption, Second-Order Nonlinear Optics, and Luminescence Properties of a Multifunctional srs-Type Metal–Organic Framework Built by Tris(4-carboxylphenylduryl)amine

Yan-Ping He, Yan-Xi Tan, and Jian Zhang*

State Key Laboratory of Structural Chemistry, Fujian Institute of Research on the Structure of Matter, Chinese Academy of Sciences, Fuzhou, Fujian 35002, China

Supporting Information

ABSTRACT: A chiral 8-fold interpenetrating srs-type metal–organic framework **FIR-28** (FIR denotes Fujian Institute of Research) exhibits a surface area of 1029 m^2/g and high C_3H_8/CH_4 separation capacity in excess of 154 and displays strong powder second-harmonic-generation efficiency, with more than half over potassium dihydrogen phosphate powder. Moreover, the luminescence properties of **FIR-28** are dependent on the solvent guests.

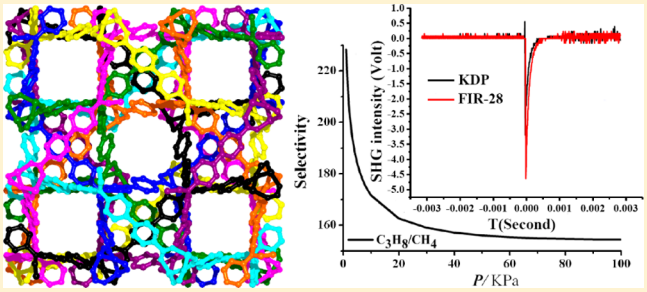

INTRODUCTION

Multifunctional metal–organic frameworks (MOFs) have attracted a great deal of chemists' attention, attributed to their fascinating structural topologies and potential applications in the fields of sorption/separation,[1] nonlinear optics (NLO),[2] fluorescence,[3] etc. To construct multifunctional MOFs,[4] the selection of the ligand is very important. As a long trigonal bridging ligand, tris(4-carboxylphenylduryl)amine (H_3TPA) can be considered as a remarkable organic precursor for the preparation of multifunctional MOFs.[5−9] For this aim, some reasonable excuses that have been considered in this context include the following: (1) The long arm (~10 Å) of the C_3-bridging H_3TPA ligand makes it easily to build highly porous MOFs for gas sorption and separation. (2) The triphenylamine core features a three-coordinated N chromophore and adopts a propeller-like conformation to minimize repulsive interactions between its phenyl rings (Figure 1). Thus, H_3TPA is a potential chiral substrate derived from a helix. (3) The vacant low-lying $2p_\pi$ orbital on the N center makes the triphenylamine derivatives good electron acceptors, leading to its potential application in the fields of NLO and fluorescence. Therefore, triphenylamine-derived multiple ligands like H_3TPA provide huge applied potential for building chiral MOFs with fascinating optoelectric properties and other new functions.

In our previous works, the H_3TPA ligand has been employed to synthesize a series of **FIR-*n*** MOFs.[6−9] For example, **FIR-7** showed a high Langmuir surface area of 1894.1 m^2/g and a C_3H_8/CH_4 separation selectivity of 78.8.[7] The second-harmonic-generation (SHG) efficiencies of **FIR-8** and **FIR-12** were about 8 and 3 times that of a potassium dihydrogen phosphate (KDP) powder.[8] **FIR-17** with a flexible framework could be used as a promising solvent sensor and exhibited reversible fluorescence switching dependent on the molecule sizes.[9] Herein, we report the synthesis, structures, gas sorption/separation, second-order NLO, and luminescence properties of a homochiral 8-fold interpenetrating srs-type MOF based on the H_3TPA ligand, namely, $Zn_2(TPA)(H_2O)_2\cdot NO_3\cdot EtOH\cdot 2DEF$ (**FIR-28**; EtOH = ethanol; DEF = *N*,*N*-diethylformamide).

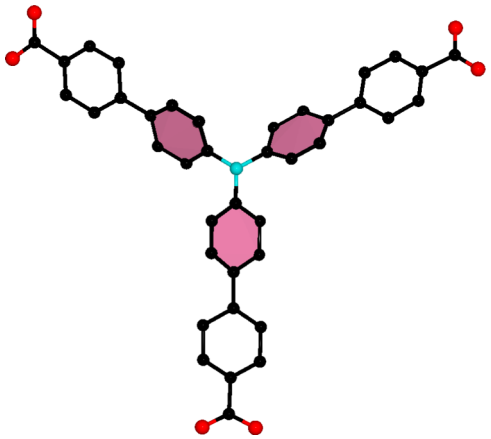

Figure 1. Structure of the H_3TPA ligand showing a propeller-like conformation.

EXPERIMENTAL SECTION

Materials and Instrumentation. All chemical reagents were obtained from commercial sources and used without further purification. Thermogravimetric analysis (TGA) was performed under a N_2 atmosphere using a Netschz STA-449C thermogravimetric

Received: May 7, 2015
Published: June 23, 2015

DOI: 10.1021/acs.inorgchem.5b01023
Inorg. Chem. 2015, 54, 6653−6656

analyzer with a heating rate of 10 °C/min. Elemental analysis (EA; C, H, and N) was carried out on a Vario Micro E III analyzer. Powder X-ray diffraction (PXRD) data were collected on the Rigaku Dmax2500 diffractometer using Cu Kα radiation (λ = 1.54056 Å) at a scan speed of 5°/min. The IR spectra (KBr pellets) were recorded on a Magna 750 FT-IR spectrophotometer. Gas-adsorption measurements were performed in an Accelerated Surface Area and Porosimetry 2020 (ASAP 2020) System (Micromeritics Instrument Ltd.). Fluorescence spectra were carried out on a Horiba Jobin-Yvon FluoroMax-4 spectrometer. NLO properties were measured by a Kurtz–Perry powder SHG test using a Q-switched Nd:YAG laser (1064 nm).

Synthesis of FIR-28. A total of 0.2 mmol (60 mg) of $Zn(NO_3)_2 \cdot 6H_2O$ and 0.1 mmol (60 mg) of H_3TPA were dissolved in a DEF/EtOH (4:1, v/v) mixed solvent and then placed in a 20 mL vial. The mixture was heated at 100 °C for 96 h and then cooled to room temperature. Yellow and polyhedral crystals were obtained and washed with DEF several times. Yield: 45% based on H_3TPA. Elem anal. for $C_{51}H_{56}N_4O_{14}Zn_2$ (**FIR-28**). Calcd: C, 56.72; H, 5.22; N, 5.19. Found: C, 56.41; H, 5.37; N, 5.23.

Crystal Data for FIR-28: space group *F*432, cubic, a = 34.7360(6) Å, V = 41912.1(13) Å^3, T = 293(2) K, Z = 32, 55591 reflections measured, 3107 independent reflections (R_{int} = 0.0458). The final R1 value was 0.0692 [$I > 2\sigma(I)$]. The final wR2(F^2) value was 0.2240 [$I > 2\sigma(I)$]. The goodness of fit on F^2 was 1.112. The structure was solved by direct methods and refined by full-matrix least squares on F^2 using the *SHELXTL-97* program. The *SQUEEZE* routine of the *PLATON* software suite was used to remove the highly disordered solvent molecules of compound **FIR-28**.

RESULTS AND DISCUSSION

A 3D open MOF, **FIR-28**, with a cationic and chiral **srs** network, was synthesized by the self-assembly of $Zn(NO_3)_2 \cdot 6H_2O$ and H_3TPA in a DEF/EtOH (4:1, v/v) mixed solvent at 100 °C for 96 h. **FIR-28** crystallized in the chiral cubic space group *F*432, which was confirmed by a single-crystal X-ray diffraction study. The asymmetric unit contains one-third of a formula unit, as shown in Figure S1 in the Supporting Information (SI). In **FIR-28**, each Zn center is four-coordinated to three carboxylate O atoms from three TPA ligands and one terminal water molecule, forming a distorted tetrahedral geometry. Each carboxylate group from the TPA linker coordinates in a bidentate fashion to a dizinc unit. The average dihedral angle between the internal phenyl plane and the N plane is 43.9°, and that between the two near phenyl plane is 21.5°. The adjacent Zn1 and Zn2 atoms are connected by three carboxylate groups to form a dimeric $[Zn_2(COO)_3(H_2O)_2]$ cluster with a Zn···Zn distance of 3.520 Å. The dimeric $[Zn_2(COO)_3(H_2O)_2]$ cluster as the basic building block lies on a crystallographic C_3 axis and further bridges six adjacent dimers through three TPA ligands, inducing a 3D open framework with a (10,3)-connecting srs topology by inducing each $[Zn_2(COO)_3(H_2O)_2]$ cluster and each TPA ligand as a 3-connected node, respectively (Figure 2a,d). All of the ligands are ranked neatly along each direction and the distance between two adjacent ligands is about 34.7 Å. In such an independent net, there are two kinds of chiral 1D tubular channels, pores A and B viewed along the *c* axis (Figure 2b,c). Pore A as a rhombic 1D channel is constructed by the right-handed helix, while the hexagonal 1D channel of pore B is built from the left-handed helix. A pair such as the srs network is interwoven to generate an opening of ~33 × 14 Å^2 (Figure S2 in the SI). Such unusually large cavities induce 8-fold interpenetration of the framework. However, the structure generates a 1D channel with a window size of about 7 Å along the *c* axis (Figure 2e). Calculated by the *PLATON* program, the

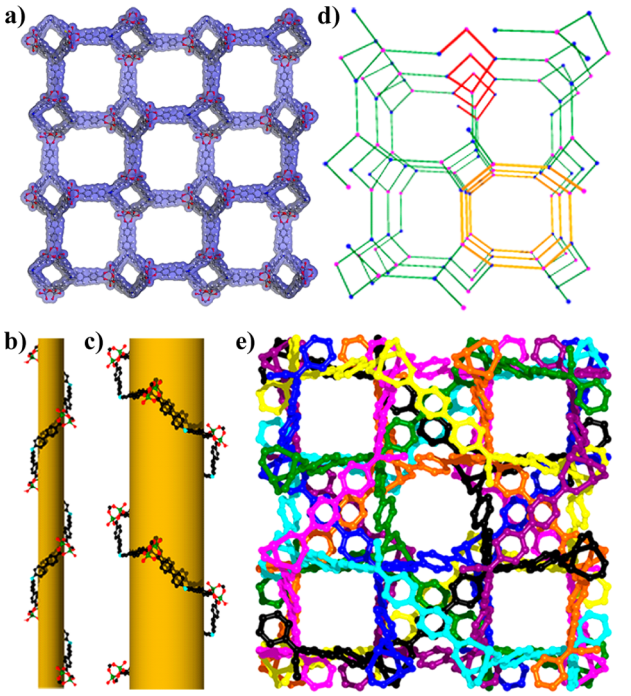

Figure 2. (a) Single framework in **FIR-28**, (b) P-helix, (c) M-helix, (d) 3-connected srs network in **FIR-28**, and (e) 8-fold interpenetrating framework of **FIR-28**.

free space in the structure of **FIR-28** without guest molecules and NO_3^- anions is about 43.9%, which is much higher than that (20.0%) of another 8-fold srs network reported by Cui's group.[10] The channels are occupied by dissociative guest molecules, all of which are calculated by EA and TGA.

As shown in Figure S3 in the SI, the TGA curve for **FIR-28** shows a weight loss of 23.2% from 30 to 280 °C, corresponding to the release of solvent guests. PXRD measurement confirmed the phase purity of **FIR-28** (Figure S4 in the SI).

In order to investigate the gas-sorption properties, **FIR-28** was exchanged by CH_2Cl_2 for 1 week and then evacuated at room temperature overnight in a vacuum to form the desolvated sample **FIR-28-ht**. At 77 K, the N_2-sorption isotherm of **FIR-28-ht** shows a typical type I behavior with significant sorption hysteresis (Figure 3), suggesting the presence of permanent micropores in **FIR-28-ht**. The N_2 uptake capacity of **FIR-28-ht** reaches 259.4 cm^3/g at 1 bar

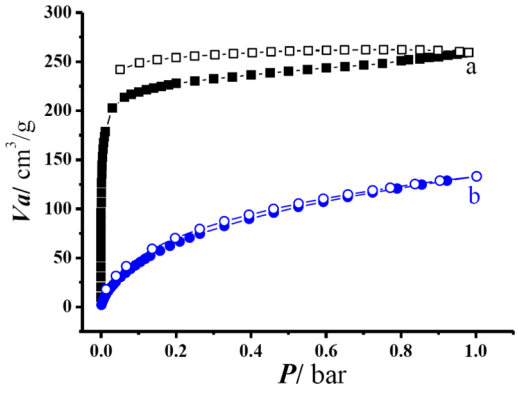

Figure 3. Gas-sorption isotherms for **FIR-28-ht** at 77 K: (a) N_2; (b) H_2.

DOI: 10.1021/acs.inorgchem.5b01023
Inorg. Chem. 2015, 54, 6653–6656

(Figure 3a). The Brunauer–Emmett–Teller and Langmuir surface areas are 737 and 1029 m^2/g, respectively. In addition, the measured pore volume of 0.401 cm^3/g (P = 0.98 bar) is slightly lower than the calculated value (0.452 cm^3/g) from the crystal structure. These results further demonstrate the stability of the activated **FIR-28-ht** framework, showing the rigidity of the host framework. The H_2 uptake capacity of 133.0 cm^3/g (1.19 wt %) is equivalent to those of previously reported for **FIR-7** and **FIR-8** (Figure 3b).[7,8]

The single-component sorption isotherms of CO_2 and different hydrocarbons for **FIR-28-ht** at 298 K are also measured. The uptakes of CO_2, C_3H_8, C_2H_4, and CH_4 for **FIR-28-ht** are 37.9, 76.5, 55.3, and 15.3 cm^3/g at 298 K and 1 bar (Figure 4), respectively. Although these values are

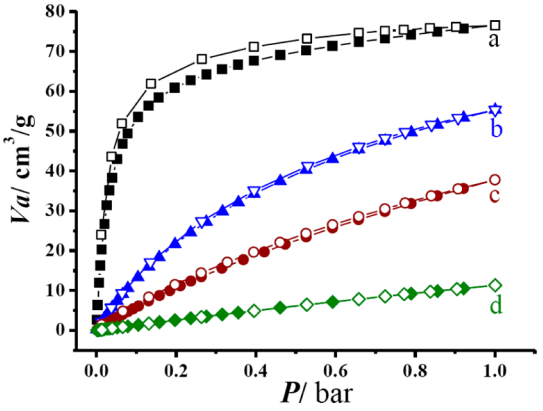

Figure 4. Gas-sorption isotherms for **FIR-28-ht** at 298 K: (a) C_3H_8; (b) C_2H_4; (c) CO_2; (d) CH_4.

significantly lower than those of MOF-74,[11] UTSA-35a,[12] UTSA-36a,[13] and FIR-7,[7] **FIR-28-ht** shows significant gas separation. The fits of experimental isotherm data to the single-site Langmuir–Freundlich mode are shown in Figure S5 in the SI. The adsorption selectivities for equimolar mixture adsorption of CO_2 and various hydrocarbons with respect to CH_4 are calculated using ideal solution adsorbed theory (IAST). The selectivities of C_3H_8/CH_4, C_2H_4/CH_4, and CO_2/CH_4 for **FIR-28-ht** are in excess of 154, 11.7, and 4.8, respectively (Figure 5). It is worth noting that the C_3H_8/CH_4 separation selectivity of **FIR-28-ht** is much higher than that of UTSA-35a (>80) reported by Chen.[12] The result indicates that

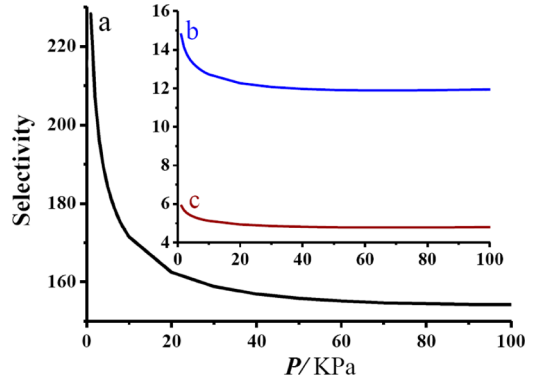

Figure 5. IAST adsorptive selectivities for **FIR-28-ht** at 298 K: (a) C_3H_8/CH_4; (b) C_2H_4/CH_4; (c) CO_2/CH_4.

FIR-28-ht may be a potential candidate for C_3H_8/CH_4 separation.

Second-order NLO was performed to further confirm **FIR-28** in the noncentrosymmertric space group *F*432. The SHG property was measured on the powder sample, using 1064 nm radiation and KDP as a reference. As shown in Figure 6a, **FIR-**

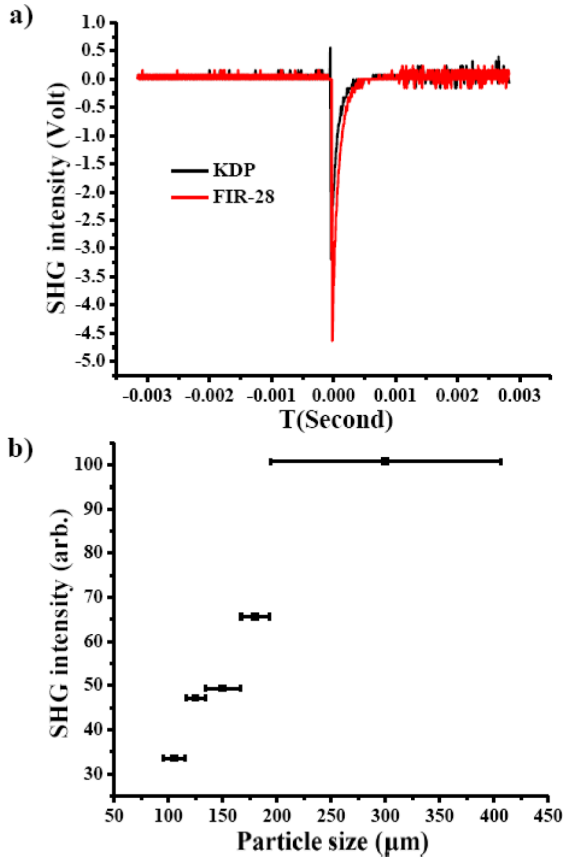

Figure 6. (a) Oscilloscope traces of the SHG signal for KDP and **FIR-28** (100–200 μm) and (b) phase-matching curve for **FIR-28**.

28 displays a strong SHG efficiency of approximately 1.5 times that of KDP powder at the same particle size (100–200 μm). By contrast, the SHG intensity for **FIR-28** is slightly higher than that of a 5-fold interpenetrating dia network reported by Liu.[14] The phase-matching curve is shown in Figure 6b. Obviously, the results accord closely with the prediction that the SHG efficiencies increase with increasing sample sizes. Furthermore, **FIR-28** can be stable in air, leading to its potential application as a second-order NLO material.

The room temperature solid-state emission spectra of the H_3TPA ligand and **FIR-28** are also studied. The free H_3TPA ligand exhibits the maximum absorption emission peak at 494 nm (Figure S6 in the SI), which belongs to the $\pi^* \rightarrow$ n or $\pi^* \rightarrow \pi$ transition. Obviously, **FIR-28** has a peak similar to that of the ligand with emission maxima at 490 nm (Figure S7 in the SI). In order to further confirm the effect of solvent guests on the fluorescent properties, the solid-state fluorescent properties of **FIR-28** containing different solvents (named **FIR-28-solvent**) were also studied at room temperature. Compared to **FIR-28**, the fluorescent intensity of **FIR-28-solvent** appeared to have different degrees of decrease (Figure 7). Acetonitrile (MeCN) has the most significant influence on the luminescence intensity, which almost disappeared when **FIR-28**

DOI: 10.1021/acs.inorgchem.5b01023
Inorg. Chem. 2015, 54, 6653–6656

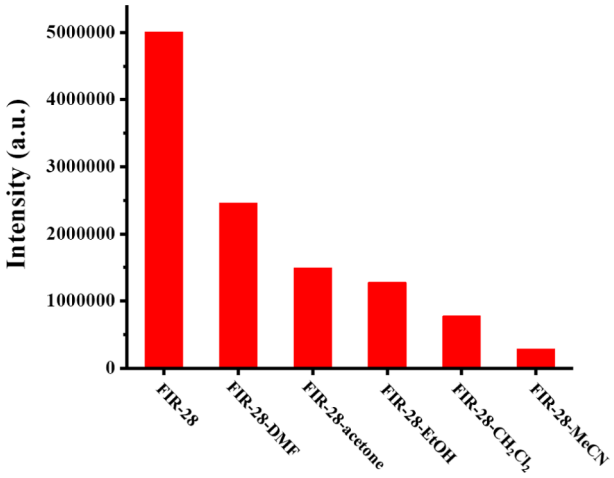

Figure 7. Transition intensities of solid **FIR-28** in different pure solvents (λ_{ex} = 360 nm).

was immersed in pure MeCN. Such a solvent-dependent luminescence property is very important for the selective sensing of MeCN molecules.[15]

CONCLUSION

In summary, chiral **FIR-28** exhibits an 8-fold interpenetrating srs-type network and displays high C_3H_8/CH_4 separation capacity. In addition, **FIR-28** displays strong powder SHG efficiency, approximately 1.5 times that of a KDP powder. Moreover, the luminescence properties of compound **FIR-28** are dependent on the solvent guest in the pores for selective sensing. All results demonstrated that **FIR-28** is a multifunctional material for potential applications.

ASSOCIATED CONTENT

Supporting Information

Additional figures, TGA, PXRD, luminescence, gas-sorption isotherms, IR spectra, and a CIF file (CCDC 1063393). The Supporting Information is available free of charge on the ACS Publications website at DOI: 10.1021/acs.inorgchem.5b01023.

AUTHOR INFORMATION

Corresponding Author

*E-mail: zhj@fjirsm.ac.cn. Tel: (+86)-591-83715030. Fax: (+86)-591-83714946.

Notes

The authors declare no competing financial interest.

ACKNOWLEDGMENTS

We are thankful for support of this work by the Chinese Academy of Sciences (Grant XDA07070200), National Science Foundation of China (Grants 21403235, 21425102, 21221001, and 91222105), and 973 program (Grant 2012CB821705).

REFERENCES

(1) (a) He, Y. B.; Zhou, W.; Qian, G. D.; Chen, B. L. *Chem. Soc. Rev.* **2014**, *43*, 5657−5678. (b) Suh, M. P.; Park, H. J.; Prasad, T. K.; Lim, D. W. *Chem. Rev.* **2012**, *112*, 782−835. (c) Zhang, Y.-B.; Furukawa, H.; Ko, N.; Nie, W. X.; Park, H. J.; Okajima, S.; Cordova, K. E.; Deng, H. X.; Kim, J.; Yaghi, O. M. *J. Am. Chem. Soc.* **2015**, *137*, 2641−2650. (d) Alsmail, N. H.; Suyetin, M.; Yan, Y.; Cabot, R.; Krap, C. P.; Lü, J.; Easun, T. L.; Bichoutskaia, E.; Lewis, W.; Blake, A. J.; Schröer, M. *Chem.—Eur. J.* **2014**, *20*, 7317−7324. (e) Xie, Y. B.; Yang, H.; Wang, Z. Y. U.; Liu, Y. Y.; Zhou, H.-C.; Li, J.-R. *Chem. Commun.* **2014**, *50*, 563−565. (f) Liu, T.-F.; Feng, D. W.; Chen, Y.-P.; Zou, L. F.; Bosch, M. T.; Yuan, S.; Wei, Z. W.; Fordham, S.; Wang, K. C.; Zhou, H.-C. *J. Am. Chem. Soc.* **2015**, *137*, 413−419. (g) Feng, D. W.; Wang, K. C.; Su, J.; Liu, T.-F.; Park, J.; Wei, Z. W.; Bosch, M.; Yakovenko, A.; Zou, X. D.; Zhou, H.-C. *Angew. Chem., Int. Ed.* **2015**, *127*, 151−156.

(2) (a) Xiong, W.-W.; Athersh, E. U.; Ng, Y. T.; Ding, J.; Wu, T.; Zhang, Q. *J. Am. Chem. Soc.* **2013**, *135*, 1256−1259. (b) Yu, J. C.; Cui, Y. J.; Wu, C. D.; Yang, Y.; Wang, Z. Y.; O'Keeffe, M.; Chen, B. L.; Qian, G. D. *Angew. Chem., Int. Ed.* **2012**, *124*, 10694−10697. (c) Reinsch, H.; van der Veen, M. A.; Gil, B.; Marszalek, B.; Verbiest, T.; de Vos, D.; Stock, N. *Chem. Mater.* **2013**, *25*, 17−26. (d) Chen, N.; Li, M.-X.; Yang, P.; He, X.; Shao, M.; Zhu, S.-R. *Cryst. Growth Des.* **2013**, *13*, 2650−2660.

(3) (a) Hu, Z. C.; Deibert, B. J.; Li, J. *Chem. Soc. Rev.* **2014**, *43*, 5815−5840. (b) Cui, Y.; Yue, Y.; Qian, G.; Chen, B. *Chem. Rev.* **2012**, *112*, 1126−1162. (c) Ni, W.-X.; Qiu, Y.-M.; Li, M.; Zheng, J.; Sun, R. W.-Y.; Zhan, S.-Z.; Ng, S. W.; Li, D. *J. Am. Chem. Soc.* **2014**, *136*, 9532−9535. (d) Sun, J.-K.; Chen, C.; Cai, L.-X.; Ren, C.-X.; Tan, B.; Zhang, J. *Chem. Commun.* **2014**, *50*, 15956−15959.

(4) (a) Lu, W. G.; Wei, Z. W.; Gu, Z.-Y.; Liu, T.-F.; Park, J.; Park, J.; Tian, J.; Zhang, M. W.; Zhang, Q.; Gentle, T., III; Bosch, M.; Zhou, H.-C. *Chem. Soc. Rev.* **2014**, *43*, 5561−5593. (b) Manna, K.; Zhang, T.; Greene, F. X.; Lin, W. B. *J. Am. Chem. Soc.* **2015**, *137*, 2665−2673. (c) Chen, Y.-P.; Liu, Y. G.; Liu, D. H.; Bosch, M.; Zhou, H.-C. *J. Am. Chem. Soc.* **2015**, *137*, 2919−2930. (d) Lin, Q. P.; Bu, X. H.; Kong, A. G.; Mao, C. Y.; Zhao, X.; Bu, F.; Feng, P. P. *J. Am. Chem. Soc.* **2015**, *137*, 2235−2238. (e) Xiong, W. W.; Zhang, Q. C. *Angew. Chem. Int. Ed.* **2015**, DOI: 10.1002/ange.201502277. (f) Gao, J. K.; Miao, J. W.; Li, P.-Z.; Teng, W. Y.; Yang, L.; Zhao, Y. L.; Liu, B.; Zhang, Q. C. *Chem. Commun.* **2014**, *50*, 3786−3788. (g) Lu, H.-S.; Bai, L. L.; Xiong, W.-W; Li, P. Z.; Ding, J. F.; Zhang, G. D.; Wu, T.; Zhao, Y. L.; Lee, J.-M.; Yang, Y. H.; Geng, B. Y.; Zhang, Q. C. *Inorg. Chem.* **2014**, *53*, 8529−8537. (h) Gao, J. K.; Ye, K. Q.; Yang, L.; Xiong, W.-W.; Ye, L.; Wang, Y.; Zhang, Q. C. *Inorg. Chem.* **2014**, *53*, 691−693.

(5) Park, H. J.; Lim, D.-W.; Yang, W. S.; Oh, T.-R.; Suh, M. P. *Chem.—Eur. J.* **2011**, *17*, 7251−7260.

(6) (a) Tan, Y.-X.; He, Y.-P.; Zhang, J. *Cryst. Growth Des.* **2012**, *12*, 2468−2471. (b) He, Y.-P.; Tan, Y.-X.; Wang, F.; Zhang, J. *Inorg. Chem.* **2012**, *51*, 1995−1997. (c) He, Y.-P.; Tan, Y.-X.; Zhang, J. *Inorg. Chem.* **2012**, *51*, 11232−11234. (d) He, Y.-P.; Tan, Y.-X.; Zhang, J. *Cryst. Growth Des.* **2013**, *13* (1), 6−9.

(7) He, Y.-P.; Tan, Y.-X.; Zhang, J. *Chem. Commun.* **2013**, *49*, 11323−11325.

(8) He, Y.-P.; Tan, Y.-X.; Zhang, J. *Inorg. Chem.* **2013**, *52*, 12758−12762.

(9) He, Y.-P.; Tan, Y.-X.; Zhang, J. *J. Mater. Chem. C* **2014**, *2*, 4436−4441.

(10) Liu, Y.; Xuan, W. M.; Zhang, H.; Cui, Y. *Inorg. Chem.* **2009**, *48*, 10018−10023.

(11) (a) Bae, Y.-S.; Lee, C. Y.; Kim, K. C.; Farha, O. K.; Nickias, P.; Hupp, J. T.; Nguyen, S. T.; Snurr, R. Q. *Angew. Chem., Int. Ed.* **2012**, *51*, 1893−1896. (b) He, Y.; Krishna, R.; Chen, B. *Energy Environ. Sci.* **2012**, *5*, 9107−9120.

(12) He, Y.; Zhang, Z.; Xiang, S.; Fronczek, F. R.; Krishna, R.; Chen, B. *Chem. Commun.* **2012**, *48*, 6493−6495.

(13) Das, M. C.; Xu, H.; Xiang, S. C.; Zhang, Z. J.; Arman, H. D.; Qian, G. D.; Chen, B. L. *Chem.—Eur. J.* **2011**, *17*, 7817−7822.

(14) Wang, Y.-L.; Fu, J.-H.; Wei, J.-J.; Xu, X.; Li, X.-F.; Liu, Q.-Y. *Cryst. Growth Des.* **2012**, *12*, 4663−4668.

(15) (a) Zhou, J.-M.; Shi, W.; Li, H.-M.; Li, H.; Cheng, P. *J. Phys. Chem. C* **2014**, *118*, 416−426. (b) Liu, K.; Shi, W.; Cheng, P. *Dalton Trans.* **2011**, *40*, 8475−8490.

DOI: 10.1021/acs.inorgchem.5b01023
Inorg. Chem. 2015, 54, 6653−6656